33rd Annual International Conference of the IEEE EMBS
Boston, Massachusetts USA, August 30 - September 3, 2011

Efficient Magnetic Torque Transduction in Biological Environments using Tunable Nanomechanical Resonators

Hooman Javaheri, Bernardo Barbiellini, and Guevara Noubir

Abstract— **Electromagnetic interactions with biological systems promise new possibilities in medical applications and synthetic biology. Creating a controlled action in biological systems requires an efficient transduction of the electromagnetic energy to thermal or mechanical biosignals. In this paper, we present the design and optimization for a nano-scale magnetic torque transducer based on a tunable nanomechanical resonator. Operating in the resonance regime allows the presented system to efficiently absorb a large amount of energy from the source. In addition, systems tuned on well separated resonance frequencies may operate simultaneously without any interference. We describe the theoretical model of the system and show the possibility of achieving the resonance in biological settings for a system with reasonable dimensions.**

I. Introduction

Remote interaction with biological systems has the potential to enable a large number of applications such as the investigation of mechanical properties of the cell and molecular signalling pathways (e.g., through targeted actuation of mechano-sensitive and thermo-sensitive ion channels), the modulation of cell functions, and controlled drug delivery [2], [3], [4], [5].

We propose a design for a passive nano-scale wireless receiver that can operate in a viscous bio-material and that can be tuned within a wide range of radio frequencies (100s MHz - few GHz). The receiver is composed of an integrated magnetic nanoparticle with a carbon nanotube. We show through theoretical analysis that such a receiver can effectively resonate with radio frequency signals and efficiently transduce the high frequency magnetic torque into actuation (e.g., 100nm carbon nanotube bound to 100nm magnetic nanoparticle can resonate at ~ 150 MHz). This is made possible thanks to advances in the manufacturing of carbon-nanotubes and magnetic nanoparticles. Tunable resonance at high frequency is the key in enabling multiplexed interactions and more sophisticated targeted actuations.

Nano-resonators have received significant attention in the last few years. However, most previous work investigates mechanisms operating in vacuum and relying on the effects of electrical fields [9], [13], [10]. The viscosity of biological tissue and its interaction with the electrical field make such approaches impractical for resonance at high frequencies. Similar resonators with a ferromagnetic tip mounted on a mechanical cantilever have been used in vibrating cantilever magnetometry [6], [7]. The interaction of electro-magnetic fields with magnetic particles in biological settings was partially investigated in [1], [8]. However, such studies only considered the effects of extremely low frequency fields, which resulted in considering the over-damped regime and overlooking the possibility of a high-frequency resonator. Finally, non-resonating transduction of relatively high frequency electromagnetic fields (i.e., 100s KHz) into actuation was investigated using the AC susceptibility of magnetic nanoparticles but showed very limited efficiency (i.e., 10^{-5} of the energy is transduced into actuation the remaining was dissipated as heat) [11], it was however utilized for targeted hypothermia against cancerous cells [12].

The structure of this paper is as follows. Section II presents the basic theoretical model of the system. The kinetic and fluid dynamics analysis is presented and the necessary conditions to achieve resonance are derived. Section III presents the design considerations along with numerical design examples. Section IV discusses the results and Section V concludes the paper. In the following sections, boldface letters represent vectors. For a given vector $\mathbf{v}$, $\mathbf{e_v}$ denotes a unit vector of its direction and v denotes its magnitude.

II. Theoretical Model

The resonator considered in this design consists of a multi-wall carbon nanotube (MWCNT) cantilever, which is clamped to the surface, and firmly attached to a spherical magnetic nanoparticle (MNP) on the free end. An alternating external magnetic field exerts a magnetic torque on the MNP creating an elastic deflection in CNT (See Fig. 1).

In this section, we provide a detailed theoretical analysis for the aforementioned resonator. First, to simplify the theoretical analysis, we propose the following set of assumptions:

- The deflection of the cantilever beam is generally a three-dimensional problem. However, we reduce the problem to 2-D by neglecting the Poisson's ratio of zero ($\nu = 0$).
- We consider *small deflections* of the cantilever beam ($\sin\theta = \theta$).
- Forces and torques due to gravity and geomagnetic field are neglected.
- The MNP is a single-domain magnetic particle of magnetite (Fe_3O_4) with a permanent magnetic moment, therefore showing no *superparamagnetic* behavior.
- We neglect the cantilever's mass since it is much smaller than the mass of MNP.
- We do not consider any plastic deformation in the cantilever, hence we have completely elastic deflections.

Hooman Javaheri and Guevara Noubir are with the College of Computer and Information Science, Northeastern University, Boston MA 02115 (Email: hooman@ccs.neu.edu, noubir@ccs.neu.edu).

Bernardo Barbiellini is with the Department of Physics, Northeastern University, Boston MA 02115 (Email: bba@neu.edu).

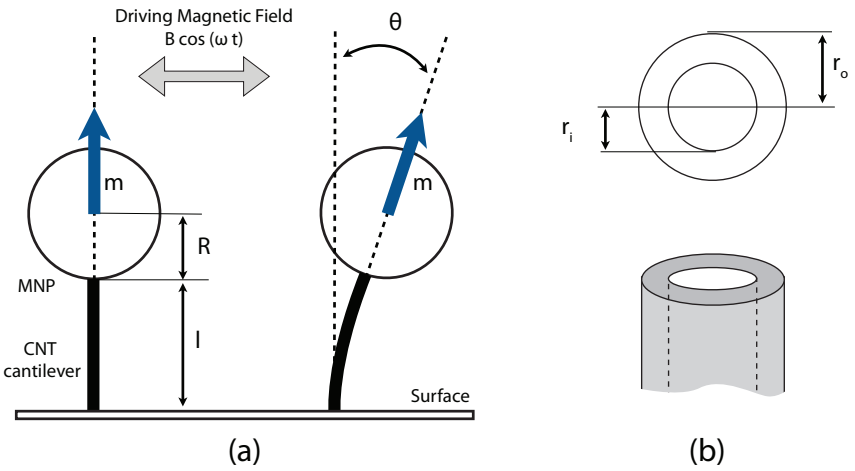

Fig. 1. The illustration of the system. (a) an overview of the components of the nanomechanical resonator at initial (Left) and operating (Right) conditions. Dimensions and angles used in the theoretical analysis are shown. (b) Cross section of the carbon nanotube cantilever.

Assume R and L denote MNP's radius and the cantilever's length, respectively. Assume the resonator sits in the xy plain. Initially, the magnetic moment of MNT, μ, aligns with the cantilever direction (y axis). A horizontal alternating magnetic field, $\mathbf{B} = B\cos(\omega t)$, provides the external magnetic torque, $\tau_\mathbf{m} = \mu \times \mathbf{B}$, to the resonator. The combination of the elastic and magnetic torques along with the dissipating torques (viscous drag forces etc.) create a damped harmonic oscillator. The equation of motion for rotational oscillations of the systems is the following:

$$I\ddot{\theta} + C\dot{\theta} + k\theta = \tau_m \tag{1}$$

where θ denotes the angular displacement of the beam, and I, C and k are the system's moment of inertia, dissipation coefficient and coefficient of elasticity resulting from the cantilever deflection, respectively.

A. General Steady-State Solution and Resonance Conditions

The natural frequency and damping ratio for a system described by Eq. 1 is as follows:

$$\omega_0 = \sqrt{\frac{k}{I}} \tag{2}$$

$$\zeta = \frac{C}{2I\omega_0} = \frac{C}{2\sqrt{kI}}. \tag{3}$$

The steady state solution for the system is given by

$$\theta(t) = \frac{\mu B}{IZ_m\omega}\cos(\omega t + \Phi), \tag{4}$$

where $Z_m(\omega) = \sqrt{(2\omega_0\zeta)^2 + (\omega_0^2 - \omega^2)^2/\omega^2}$ is the system's impedance, and $\Phi(\omega) = \arctan(2\omega\omega_0\zeta/(\omega^2 - \omega_0^2))$ is the phase shift from the driving torque.

For such an oscillator, resonance is possible if and only if $\zeta < \sqrt{2}/2$, which means the system is underdamped. The corresponding resonant frequency is given by $\omega_r = \omega_0\sqrt{1-2\zeta^2}$ at which maximum deflection, θ_{max}, occurs. Using Eq. 2 and 3, the resonance condition and the resonant frequency will be

$$C < \sqrt{2kI} \tag{5}$$

$$\omega_r = \sqrt{\frac{2kI - C^2}{2I^2}}. \tag{6}$$

For a small damping ratio (i.e. $\zeta \ll 1$, typically less than 0.05), the quality factor of the resonance equals $Q = 1/2\zeta = \sqrt{kI}/C$. This is particularly useful for determining the resonator's absorbed power. By definition,

$$Q = \omega_r \times \frac{\text{Maximum energy stored in the system}}{\text{Power absorbed by the system}}, \tag{7}$$

where the maximum energy stored in the system is given by $E_{max} = k\theta_{max}^2/2$. Finally the bandwidth (or absorption width) is $\Delta\omega = \omega_r/Q$.

B. Model-Specific Solution

In this section, we derive the equations for I, C, k, and τ_m for the presented resonator by computing the torques and moments of inertia with respect to the cantilever's base. External electromagnetic torque is given by

$$\tau_m = \mu \times \mathbf{B} = \mu B\sin(\frac{\pi}{2} - \theta)\cos(\omega t) \tag{8}$$

$$= \mu B\cos(\theta)\cos(\omega t)$$

$$= \mu B\cos(\omega t). \tag{9}$$

Neglecting the mass of the cantilever, the moment of inertia of the system equals the moment of inertia for a spherical mass (i.e. the MNP) with respect to cantilever's base, and is given by

$$I = \frac{2}{5}mR^2 + mD^2, \tag{10}$$

where m is the mass of the MNP, and $D = (l+R)$ is the distance of MNP's center of mass from the base. Therefore,

$$I = m(\frac{2}{5}R^2 + D^2) \tag{11}$$

$$= \frac{4\pi}{3}\rho R^3(\frac{2}{5}R^2 + (l+R)^2), \tag{12}$$

where ρ is the density of the magnetite.

The elasticity coefficient (i.e. equivalent spring constant) for a cantilever beam is given by Bernoulli-Euler equation. For small deflections of the beam with a torque load at the tip, we have

$$k = \frac{EI_c}{l}, \tag{13}$$

where E, I_c, and l are Young's modulus, second moment of cross-section, and length of the beam [15]. MWCNT is basically a cylinder, thus $I_c = \frac{\pi}{4}(r_o^4 - r_i^4)$ where r_o and r_i are outer and inner radii of the CNT.

Dissipation Mechanisms: Several dissipation mechanisms may affect the oscillations of the resonator. The dissipations in nanoresonators can be divided into two categories: a) *Intrinsic losses*, which are due to imperfections and interactions within the structure of the resonator (e.g. phonon-phonon interactions, thermoelastic effect). b) *Extrinsic losses*, which are the result of interactions with the surrounding environment (e.g. viscous friction, clamping losses). In this model, we only consider the extrinsic dissipations. The viscous nature of the biological media makes the viscous friction the dominant factor among the extrinsic losses. For the sake of simplicity in this paper, we only consider dissipations due to drag forces in the fluid. Small particles such as nanoresonator components have very small Reynolds number ($R_e \to 0$), thus fluid behaviour follows the Stokes' law. For a spherical object of radius R in this condition we have,

$$F_D = 6\pi R\eta v, \tag{14}$$

where η and v are fluid viscosity and velocity of the object. Substituting for $v = (l+R)\dot{\theta}$, and $C = \tau_D/\dot{\theta}$, we have

$$\begin{aligned} C &= \frac{\tau_D}{\dot{\theta}} = \frac{F_D \times (l+R)}{\dot{\theta}} \\ &= 6\pi R\eta (l+R)^2. \end{aligned} \tag{15}$$

Note that because of the small moving area, the drag forces on the cantilever are negligible and not considered.

Substituting from Eq. 12, 13, and 15 results in the expanded form of resonance condition below:

$$54\eta^2(l+R)^4 < E\rho R(\frac{2}{5}R^2 + (l+R)^2)(r_o^4 - r_i^4). \tag{16}$$

III. Design and Optimization

Having explored the theoretical model for the system, this section discusses the design and optimization of the system. The goal is to design and to optimize a resonator that operates at a given resonant frequency in a given microenvironment. Identifying the key parameters of the design is necessary to achieve the desired performance. The equations derived in the preceding section include two different types of parameters. First are the *material properties*, which include Young's modulus (E), density (ρ), and viscosity of the microenvironment (η). Second are *structural parameters*, which are MNP radius (R), CNT length (l), and radii (r_o and r_i). Adjusting the material properties could potentially require radical changes in the design and setup and might not be possible at all. In contrast, structural parameters provide much wider range of flexibility, thus make good tuning parameters for the resonator.

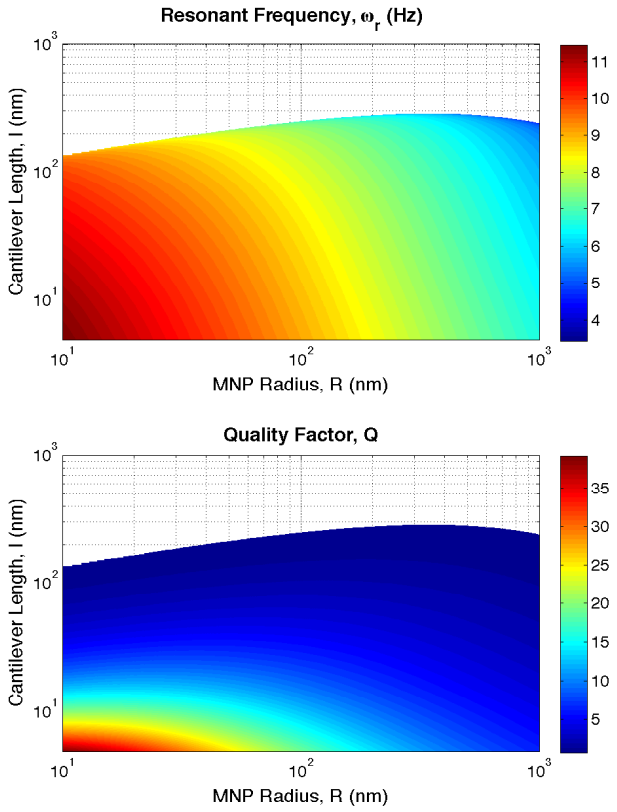

Fig. 2. (Color online) Resonant frequency ω_r (upper graph) and Quality factor (lower graph) for reasonable range of values for MNP radius (10 nm $< R <$ μm) and CNT length (5 nm $< l <$ μm). The points located outside the colored region represent overdamped oscillations. Graphs are generated in MATLAB.

A numerical example for design and optimization of a real world system is presented below. Note that in this example R and l serve as tuning parameters and the rest of the parameters are given as follows: MNP is made of magnetite (Fe_3O_4) with desity of $\rho = 5200$ Kg/m^3. The cantilever beam is a carbon nanotube with Young's modulus of $E = 5$ TPa, and outer and inner radii of $r_o = 5$ nm, $r_i = 2$ nm, respectively. The system will be installed in an aqueous environment, therefore $\eta = 10^{-3}$ Pa.s . Finally, the overall size of the system should stay within reasonable range for biological application (i.e. less than few micrometers).

We first look at the possibility of the resonance for such a system. The resonance happens provided that the inequality presented in Eq. 16 is fulfilled. Fig. 2 shows the resonant frequency and quality factor for the system for reasonable values of R and l. Data from Fig. 2 suggests that resonant conditions are achievable for a large range of tuning parameters (Colored region).

The next step is to find the optimal configuration (or an

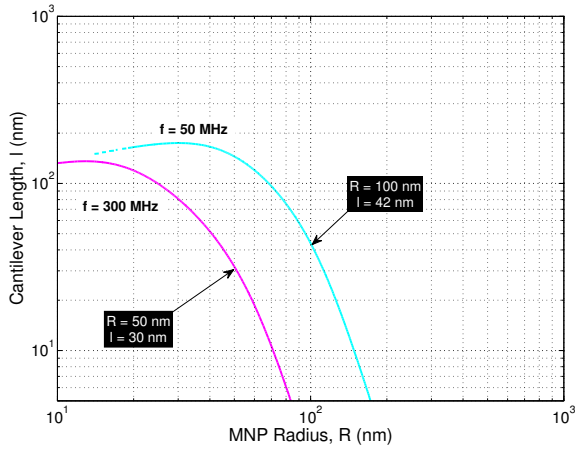

Fig. 3. (Color online) Optimization look-up graph for a magnetite/(5,2)-CNT resoator operating in water at 60 MHz (blue line) and 300 MHz (purple). Any point on an specific frequency line is a valid configuration for R and l, which results in a resonator with resonant frequency of the line's nominal frequency. Graph is generated in MATLAB.

optimal set of configurations) in which the resonator operates at desired resonant frequency. This is possible by determining the cross section of the graph of resonant frequency as a function of R and l at given frequency. Operating at a frequency is not possible if the cross section is empty. Otherwise, each point on the cross section represents a valid configuration in which the resonator operates at the desired frequency. Fig 3 illustrates this process for our numerical example. As shown on the graph, ($R = 100$nm, $l = 42$nm) configuration leads to resonant frequency of $f_r = 50$ MHz, while $f_r = 300$ MHz can be achieved by choosing ($R = 50$nm, $l = 30$nm). These are reasonable values in today's manufacturing technology.

IV. Discussion

The tiny size of nanoresonators significantly limits their amount of energy. With such limited energy budget, overcoming the ambient thermal noise (i.e. k_BT, where k_B is the Boltzmann constant and T is the temperature in Kelvin.) becomes a challenging obstacle. In order to have a meaningful impact on the surrounding microenvironment, the total energy of the resonator must exceed k_BT. This determines the *sensitivity* of the resonator to external actuations.

Another important challenge is the mechanism by which the CNT is attached to the MNP. A very strong (covalent) bond is required to achieve good performance. While the process of attaching an MNP to a CNT is still underexplored, recent research demonstrates manufacturing similar bonds by chemically modifying the surface of MNPs and CNTs [16].

Finally, even in the case of good coupling between the nanoresonator and the external field, the oscillations eventually become non-linear. This makes the design that is only based on linear resonance flawed and not sufficient. In this work, we skipped the non-linear analysis due to the limited space.

V. Conclusions

We present a nano-scale radio-receiver that is capable of achieving resonance in biological settings. The system is based on a magnetic nanoparticle attached to a carbon nanotube cantilever. The receiver transduces the magnetic field into a radio-frequency torque. The benefit of using magnetic fields is that, unlike electric fields, they couple weakly with non-targeted biological tissues. This makes tunable resonance at fairly high frequencies feasible in biological settings, therefore enabling several unique capabilities such as multiplexed interaction and targeted actuation. We conduct theoretical analysis for the system and predict the desired functionality within reasonable scale for frequency (few MHz - few GHz), carbon nanotube size (100s nm), and magnetic nanoparticles size (100s nm). We believe this will open several new avenues for research in the areas of targeted actuation of mechano-sensitive and thermo-sensitive ion channels, the modulation of cell functions, and controlled drug delivery.

Acknowledgements

This material is based upon work supported by the National Science Foundation under Grant No. CISE/CNS 0958927.

References

[1] Winklhofer and Kirschvink. A quantitative assessment of torque-transducer models for magnetoreception. Journal Of The Royal Society Interface (2010) vol. 7 pp. S273-S289
[2] Dobson. Remote control of cellular behaviour with magnetic nanoparticles. Nature nanotechnology (2008)
[3] Mannix et al. Nanomagnetic actuation of receptor-mediated signal transduction. Nature nanotechnology (2008) vol. 3 (1) pp. 36-40
[4] Chen. Remote control of living cells. Nature nanotechnology (2008)
[5] Huang et al. Remote control of ion channels and neurons through magnetic-field heating of nanoparticles. Nature Nanotechnology (2010) vol. 5 (8) pp. 602-606
[6] Stipe et al. Magnetic dissipation and fluctuations in individual nanomagnets measured by ultrasensitive cantilever magnetometry. Physical Review Letters (2001)
[7] Zhang and Hammel, Magnetic resonance force microscopy with a ferromagnetic tip mounted on the force detector, Solid State Nuclear Magnetic Resonance, Volume 11, Issues 1-2, March 1998, pp 65-72
[8] Adair. Constraints on biological effects of weak extremely-low-frequency electromagnetic fields. Physical Review A (1991) vol. 43 (2) pp. 1039-1048
[9] Jensen et al. Nanotube radio. Nano letters (2007) vol. 7 (11) pp. 3508-3511
[10] Poon et al. Optimal Frequency for Wireless Power Transmission Into Dispersive Tissue. Antennas and Propagation, IEEE Transactions on (2010) vol. 58 pp. 1739 - 1750
[11] Janssen et al. Controlled torque on superparamagnetic beads for functional biosensors. Biosensors & Bioelectronics (2009) vol. 24 (7) pp. 1937-1941
[12] Hergt et al. Magnetic particle hyperthermia: nanoparticle magnetism and materials development for cancer therapy. Journal Of Physics-Condensed Matter (2006) vol. 18 (38) pp. S2919-S2934
[13] Dykman et al. Spectrum of an Oscillator with Jumping Frequency and the Interference of Partial Susceptibilities. Physical Review Letters (2010) vol. 105 (23) pp. 230601
[14] Gupta et al. Synthesis and surface engineering of iron oxide nanoparticles for biomedical applications. Biomaterials (2005) vol. 26 (18) pp. 3995-4021
[15] Meirovitch. Fundamentals of Vibrations. McGraw-Hill (2000)
[16] Jong Hyun Choi et. al. Multimodal Biomedical Imaging with Asymmetric Single-Walled Carbon Nanotube/Iron Oxide Nanoparticle Complexes. Nano Letters 2007 7 (4), 861-867